only the ramp and MA(1) model, and for only the random walk and MA(1) model. Figure 7 shows that model adequacy is attained only by using the combination of two nonstationary processes and one stationary process. Note that a good fit of the data is not attained with only one nonstationary process. It can readily be seen from Eq. (4.5) that the stationary θ_1 parameter plays an important part in determining the fit of the theoretical to the empirical ensemble mean squared gyro drift rate.

It is important to note at this time that the "goodness of fit" of the theoretical mean squared gyro drift rate to the empirical ensemble mean squared gyro drift rate is based on the models and parameter values determined from the *single sample* long term gyro drift rate. The single sample time series analysis techniques give us time estimates of ensemble parameters, where the particular time series analyzed can be considered as one member of the ensemble.

5. Conclusions

The detailed methods by which one would analyze long term gyro drift rate have been presented in this paper. The motivation behind this study was to present a uniform approach for determining a mathematical model for the drift rate of a gyro that must operate in an inertial system over a prolonged period of time.

It has been demonstrated in this paper that: 1) the single sample time series analysis techniques are capable of handling random walks and ramps appearing together in time series data and 2) the technique of ensemble averaging is a useful tool in determining model adequacy, even though the model is determined from the single sample process.

References

[1] Oravetz, A. S., Jakimczyk, S. J., and Sandberg, H. J., "Mathematical Modeling of Long Term Gyro Drift Rate," *EASCON '68 Conference Proceedings*, Sept. 1968.

[2] Box, G. E. P. and Jenkins, G. M., *Statistical Models for Forecasting and Control*, Holden-Day, to be published.

[3] Jenkins, G. M. and Watts, D. G., *Spectral Analysis and Its Applications*, Holden-Day, 1968.

OCTOBER 1970 AIAA JOURNAL VOL. 8, NO. 10

Minimum-Fuel Thrust-Limited Transfer Trajectories between Coplanar Elliptic Orbits

E. A. KERN*
TRW Systems Group, Houston, Texas

AND

D. T. GREENWOOD†
The University of Michigan, Ann Arbor, Mich.

A method is developed for the computation of minimum-fuel transfer trajectories between coplanar elliptic orbits with a thrust-limited variable-mass rocket moving in a central gravitation force field. Each orbit is defined through the eccentricity, semilatus rectum, and argument of pericenter. Transfer time is left open. The minimum-fuel trajectory is assumed to consist of two thrusting phases separated by a coasting phase. Computation of the minimum-fuel transfer trajectory is accomplished by a direct integration of the rocket equations of motion and the associated adjoint equations. This direct approach is made possible by a transformation of the adjoint equations into a set of equations which provide a much better understanding of the general behavior of minimum-fuel transfer trajectories. An IBM 7094 digital computer program with primarily single-precision arithmetic is used for the computation. Rapid convergence is obtained over a broad class of transfer trajectories and rocket thrust levels.

Nomenclature

A = $ze\cos\phi$
a = ratio of maximum rocket thrust to initial rocket weight
B = $ze\sin\phi$
c = rocket effective exhaust velocity
e = orbital eccentricity
f = true anomaly
H = Hamiltonian
H_0 = a portion of the Hamiltonian
H_1 = a portion of the Hamiltonian
h = $1/r$
m = instantaneous rocket mass
p = semilatus rectum
r = distance from center of force to the rocket
s = switching function (s positive implies thrust is on)
t = time
u = radial velocity$/r$
v = transverse velocity$/r$
w = reciprocal of the instantaneous mass
z = reciprocal of the per-unit-mass angular momentum
β = $\tan^{-1}(\lambda_\theta/\nu)$

Presented as Paper 69-914 at the AIAA/AAS Astrodynamics Conference, Princeton, N.J., August 20–22, 1969; submitted August 13, 1969; revision received April 20, 1970. This paper represents a portion of E. Kern's Ph.D. thesis for the Aerospace Engineering Department, The University of Michigan. It was supported by The Air Force Institute of Technology, Wright-Patterson Air Force Base, Ohio.

* Formerly with the U.S. Air Force Institute of Technology; now member of the Technical Staff. Member AIAA.

† Professor, Aerospace Engineering Department. Associate Fellow AIAA.

θ = $f + \phi$ = total polar angle
λ = adjoint variable
Λ = $[\lambda_u^2 + \lambda_v^2]^{1/2}$
ν = $h\lambda_h$
ξ = thrust intensity control variable ($0 \leq \xi \leq 1$)
ρ = $[\nu^2 + \lambda_\theta^2]^{1/2}$
ϕ = argument of pericenter
Ψ = angle of thrust orientation above local horizontal

I. Introduction

THE problem considered here concerns the determination of time-open minimum-fuel thrust-limited transfer trajectories between coplanar elliptic orbits. That is, given two coplanar elliptic orbits defined, i.e., by pairs of semilatera recta, eccentricities and arguments of pericenter, the problem is to find the minimum-fuel transfer trajectory between these two orbits. Prior attempts to find a reliable and efficient method for solving this problem have met with only limited success because of the extreme sensitivity of the particular two-point boundary value problem. A significant contribution has been made by McCue, who used a highly sophisticated quasilinearization method to obtain solutions.[1] However, McCue's method consumes a relatively large amount of computer time and appears very difficult to program. Another pioneering effort worthy of mention was made by Handelsman who computed minimum-fuel trajectories using impulsive starting conditions.[2] Handelsman's orbit-to-orbit transfers were limited to coplanar, fixed-time, open-angle Earth-to-Mars type trajectories. The approach taken in this paper is to transform the conventional adjoint variables into a set of variables which provide more insight into the characteristics of the optimum transfer trajectory. Differential equations are developed for the transformed variables, and these equations are integrated directly along with the rocket equations of motion to find the minimum-fuel transfer trajectory. The known two-impulse transfer trajectory is used to assist in the choice of the unknown initial conditions.[3-5] A systematic approach is employed to force the set of differential equations to satisfy the boundary conditions. The transfer trajectory is assumed to consist of two thrusting phases separated by a coasting phase.

II. Necessary Conditions for Optimality

The optimal transfer trajectory must satisfy the desired initial and final boundary conditions while maximizing the final mass of the rocket. A set of necessary conditions for this optimal trajectory can be developed from variational calculus principles.

Units and Scaling

In order to obtain better scaling of the problem variables and parameters and to make the results more readily applicable to motion about any central-body attracting force, the following set of units is employed throughout the study: unit length = r^* = convenient distance from attracting center, unit acceleration = g^* = acceleration of gravity at distance r^*, and unit mass = initial mass of the rocket vehicle. As a result of this choice of units $[r^*/g^*]^{1/2}$ = unit of time (in one time unit a satellite in circular orbit of radius r^* would traverse through a central angle of one radian), $[r^*g^*]^{1/2}$ = unit of velocity (the orbital velocity of a satellite in a circular orbit of radius r^* would equal one velocity unit), and g^*r^{*2} = gravitational parameter of the central body = 1.

Equations of Motion

The differential equations defining the motion of the rocket are derived under the following assumptions: 1) The rocket is a variable mass particle. 2) Rocket thrust is always in the plane of motion, can be varied in both magnitude and direction, and is a linear function of the mass flow rate. 3) The acceleration of the rocket is due solely to the rocket thrust and a spherically symmetric inverse square central gravitational force field. With the aforementioned assumptions the rocket equations of motion are

$$\dot{h} = -uh \tag{1}$$

$$\dot{u} = v^2 - u^2 - h^3 + a\xi wh \sin\Psi \tag{2}$$

$$\dot{v} = -2uv + a\xi wh \cos\Psi \tag{3}$$

$$\dot{\theta} = v \tag{4}$$

$$\dot{w} = a\xi w^2/c \tag{5}$$

where, with r the radial distance from the center of the attracting body, $h = 1/r$, u = radial velocity/r, v = transverse velocity/r, a = ratio of maximum rocket thrust to initial rocket weight, ξ = thrust intensity control variable ($0 \leq \xi \leq 1$), w = reciprocal of the rocket mass, Ψ = angle of thrust orientation above the local horizontal, and c = rocket effective exhaust velocity.

The Hamiltonian for the system defined by Eqs. (1-5) is

$$H = -uh\lambda_h + (v^2 - u^2 - h^3)\lambda_u - 2uv\lambda_v + \lambda_\theta v + a\xi w[h(\lambda_v \cos\psi + \lambda_u \sin\psi) + w\lambda_w/c] \tag{6}$$

where λ_h, λ_u, λ_v, λ_θ, and λ_w are the adjoint variables associated with h, u, v, θ, and w, respectively.

The optimal control must be chosen to maximize the Hamiltonian. Therefore, the thrust-orientation angle must be chosen such that

$$\sin\Psi = \lambda_u/\Lambda \tag{7}$$

$$\cos\Psi = \lambda_v/\Lambda \tag{8}$$

where

$$\Lambda = [\lambda_u^2 + \lambda_v^2]^{1/2} \tag{9}$$

The Hamiltonian maximized with respect to the thrust-orientation angle becomes

$$H = -uh\lambda_h + (v^2 - u^2 - h^3)\lambda_u - 2uv\lambda_v + \lambda_\theta v + a\xi w(h\Lambda + w\lambda_w/c) \tag{10}$$

In order to maximize the Hamiltonian with respect to the thrust intensity control variable ξ, it is convenient to partition the Hamiltonian as follows

$$H = H_0 + a\xi wH_1 \tag{11}$$

where

$$H_0 = -uh\lambda_h + (v^2 - u^2 - h^3)\lambda_u - 2uv\lambda_v + \lambda_\theta v \tag{12}$$

$$H_1 = h\Lambda + w\lambda_w/c \tag{13}$$

It follows that ξ must be chosen equal to one if H_1 is greater than zero and equal to zero if H_1 is less than zero. In other words, if H_1 is positive, the rocket should be thrusting at maximum intensity while for H_1 negative, the rocket should be in a non-thrusting or coasting phase. If H_1 is zero over any finite time interval, ξ could take on any value in its permissible range without affecting the Hamiltonian. However, for the case of time-open transfer trajectories, minimum-fuel thrusting arcs for which the thrust-intensity control variable takes on intermediate values in the range 0-1 have been shown by Robbins and also Kopp and Moyer to be nonexistent.[6,7]

From the Hamiltonian of Eq. (10), the adjoint equations are

$$\dot{\lambda}_h = \lambda_h u + 3h^2\lambda_u - a\xi w\Lambda \tag{14}$$

$$\dot{\lambda}_u = \lambda_h h + 2u\lambda_u + 2\lambda_v v \tag{15}$$

$$\dot{\lambda}_v = -2\lambda_u v + 2\lambda_v u - \lambda_\cdot \tag{16}$$

$$\dot{\lambda}_\theta = 0 \tag{17}$$

$$\dot{\lambda}_w = -2a\xi w\lambda_w/c - a\xi h\Lambda \tag{18}$$

Transformation of the Adjoint Variables

The conventional adjoint variables can be replaced by a set of new variables which are coupled in a physical sense more directly to the actual transfer trajectory. The differential equations which these new variables must satisfy will be shown in the subsequent analysis. Differentiating both sides of Eqs. (7) and (8) and simplifying, it can be shown that

$$\dot{\Lambda} = 2u\Lambda + \nu \sin\Psi - \lambda_\theta \cos\Psi \tag{19}$$

$$\dot{\psi} = 2v + (\nu \cos\Psi + \lambda_\theta \sin\Psi)/\Lambda \tag{20}$$

where

$$\nu = h\lambda_h \tag{21}$$

Since the sign of H_1 controls the rocket thrusting, a switching function s can be defined as follows:

$$s = H_1/\Lambda \tag{22}$$

Λ is by definition a positive quantity. Therefore, for s positive the rocket thrust should be at maximum intensity ($H_1 > 0$), while for s negative the rocket thrust should be zero ($H_1 < 0$). Direct differentiation of Eq. (22) yields after some simplification

$$\dot{s} = (s - h)(\lambda_\theta \cos\Psi - \nu \sin\Psi)/\Lambda + uh - s(2u + a\xi w/c) \tag{23}$$

Finally, differentiating Eq. (21), the defining equation for ν, it follows from Eqs. (1) and (14) that

$$\dot{\nu} = \Lambda h(3h^2 \sin\Psi - a\xi w) \tag{24}$$

The conventional adjoint variables λ_h, λ_u, λ_v, and λ_w can now be replaced by the variables Λ, Ψ, s, and ν. Therefore, the differential equations (19, 20, 23, and 24) replace the adjoint equations (14–16 and 18). These new differential equations provide for a greater understanding of minimum-fuel trajectories.

Transformation to the z, A, B Coordinates

Since the initial and final boundary conditions on the trajectory are a set of orbital parameters, it generally proves more accurate to integrate a set of orbital parameters in place of the conventional position and velocity coordinates. The particular orbital parameters to be employed in the integration are as follows[9,10]:

$$z = h^2/v \tag{25}$$

$$A = ze \cos\phi \tag{26}$$

$$B = ze \sin\phi \tag{27}$$

These new variables can be shown to satisfy the following differential equations

$$\dot{z} = -a\xi w z^2 \cos\Psi/h \tag{28}$$

$$\dot{A} = a\xi w(\cos\theta \cos\Psi + \sin\theta \sin\Psi + z^2 \cos\Psi \cos\theta/h) \tag{29}$$

$$\dot{B} = a\xi w(\sin\theta \cos\Psi - \cos\theta \sin\Psi + z^2 \cos\Psi \sin\theta/h) \tag{30}$$

The previous three equations along with Eqs. (4, 5, 17, 19, 20, 23, and 24) are the basic set of equations which must be satisfied by the minimum fuel trajectory. This set of equations will be defined as the system equations. The variables h, u, and v, which appear in these equations, can be found from the auxiliary relations

$$\phi = \tan^{-1}(B/A) \tag{31}$$

$$e = A/(z \cos\phi) \tag{32}$$

$$p = 1/z^2 \tag{33}$$

$$f = \theta - \phi \tag{34}$$

$$h = (1 + e \cos f)z^2 \tag{35}$$

$$u = hez \sin f \tag{36}$$

$$v = h^2/z \tag{37}$$

The thrust intensity control variable ξ is determined by the switching function according to the following logic:

$$\xi = 1, s > 0 \tag{38}$$

$$\xi = 0, s < 0 \tag{39}$$

Boundary Conditions

Let the initial and final orbits be defined by the sets (p_0,e_0,ϕ_0) and (p_f,e_f,ϕ_f) which represent the semilatus rectum, eccentricity, and argument of pericenter for the initial and final orbits, respectively. Since the initial mass of the rocket is known, the boundary conditions on the state variables at the initial time t_0 and the final time t_f will be as follows

$$z(t_0) = [1/p_0]^{1/2}, z(t_f) = [1/p_f]^{1/2} \tag{40}$$

$$A(t_0) = z(t_0)e_0 \cos\phi_0, A(t_f) = z(t_f)e_f \cos\phi_f \tag{41}$$

$$B(t_0) = z(t_0)e_0 \sin\phi_0, B(t_f) = z(t_f)e_f \sin\phi_f \tag{42}$$

$$w(t_0) = 1 \tag{43}$$

The times t_0 and t_f are defined as the times at which the transfer is initiated and terminated, respectively. Defining the times in this manner eliminates the need for coast periods at the start and the finish of the computation. This results in no loss in generality since the initial and final true anomalies are not prespecified but must be determined to satisfy the two-point boundary value problem.

As a consequence of the transversality conditions and the boundary conditions on the state variables it can be shown that[8]

$$H_0(t_0) = 0: H_0(t_f) = 0 \tag{44}$$

For the time-open case being considered here, the Hamiltonian must vanish along the entire transfer trajectory. This fact along with Eq. (44) and the definition of the times t_0 and t_f leads to the boundary conditions on the switching function

$$s(t_0) = 0: s(t_f) = 0 \tag{45}$$

A boundary condition on one adjoint variable can be chosen arbitrarily. Hence, without any loss in generality, it is permissible to set

$$\Lambda(t_0) = 1 \tag{46}$$

III. Minimum-Fuel Algorithm

The minimum-fuel trajectory must satisfy the differential equations (4, 5, 17, 19, 20, 23, 24, and 28–30) and the boundary conditions given by Eqs. (40–46). To find a trajectory that satisfies this system of equations is a relatively difficult task since at the initial time, the polar angle θ, the thrust angle Ψ, the variable ν, and the adjoint variable λ_θ are unknown. The basic problem is to find that correct combination of the initial conditions for θ, Ψ, ν, and λ_θ such that when the system of differential equations is integrated, the boundary conditions at the final time are satisfied. Without any loss in generality the reference line from which all angular measurements are made can be defined to pass through pericenter of the initial orbit. Therefore, $\phi(t_0)$ will be equal to zero, and from Eq. (34), it is obvious that finding the initial polar angle $\theta(t_0)$ is equivalent to finding the initial true anomaly $f(t_0)$. The final time in this case is not fixed but can be defined as the time at which all the conditions at the end of the trajectory are satisfied.

Initial-Approximate Transfer Trajectory

The corresponding two-impulse transfer trajectory can be used as an aid in constructing a finite-thrust transfer trajectory which serves as a good first approximation to the desired transfer trajectory.[3-5] This finite-thrust transfer trajectory is defined as the initial-approximate transfer trajectory. Reasonable estimates for the initial thrust angle, initial true anomaly, and the thrusting interval durations can be easily derived from the two-impulse transfer trajectory. The initial thrust orientation angle is set equal to the thrust orientation angle for the first impulse, and the initial true anomaly is computed by conjecturing that on each thrusting phase the average true anomaly for the impulsive thrust should be equal to the true anomaly at the midpoint of the corresponding finite-thrust interval. The durations of the thrusting intervals for the initial-approximate transfer trajectory are chosen so that the integrals of rocket acceleration for the finite-thrust case are equal to the respective magnitudes of the velocity change vectors for the impulsive case.

The four unknown initial conditions $\Psi(t_0)$, $f(t_0)$, $\nu(t_0)$, and λ_θ are not independent. With three of these unknowns selected, the fourth condition is fixed through the requirement that H_0 vanish at the initial time. It has proved convenient to set independently the initial conditions on f, Ψ, and ν. Setting H_0 from Eq. (12) equal to zero and solving for λ_θ gives after some simplification

$$\lambda_\theta = \left\{ \frac{e\nu \sin f}{1 + e\cos f} - \frac{e\Lambda \sin f}{p^{1.5}} \left[\sin\Psi \frac{\cos f + e\cos 2f}{\sin f} - 2\cos\Psi(1 + e\cos f) \right] \right\}_{t=t_0} \quad (47)$$

The initial values of Ψ and ν can be chosen so that the thrusting intervals are of the desired duration. A good first approximation for $\Psi(t_0)$ is available from the two-impulse trajectory, but this value must be refined in order to achieve the desired thrusting durations. In selecting a first approximation for $\nu(t_0)$ a considerable amount of insight can be gained by writing Eqs. (19, 20, and 23) in the form

$$\dot{\psi} = 2v + \rho\cos(\Psi - \beta)/\Lambda \quad (48)$$

$$\dot{s} = (h - s)\rho\sin(\Psi - \beta)/\Lambda + hu - s(2u + a\xi w/c) \quad (49)$$

$$\dot{\Lambda} = 2u\Lambda + \rho\sin(\Psi - \beta) \quad (50)$$

where

$$\rho = [\lambda_\theta^2 + \nu^2]^{1/2} \quad (51)$$

$$\beta = \tan^{-1}[\lambda_\theta/\nu] \quad (52)$$

In order to achieve the desired switching function characteristics on the first thrusting interval, the switching function must be as shown in Fig. 1. Numerical results from the two-impulse trajectory indicate that the thrust angle should always be near either 0° or 180° on the thrusting intervals. This has been verified analytically by Culp.[11] With $\Psi(t_0)$ limited in the previous manner, a closer examination of Eqs. (48) and (49) indicates that for the switching function to exhibit the proper characteristics on the first thrusting interval, $\nu(t_0)$ must be restricted to the following ranges of values.[8]

$$[\nu(t_0)]_{\Psi(t_0)\approx 0^\circ} < 0 \quad (53)$$

$$[\nu(t_0)]_{\Psi(t_0)\approx 180^\circ} > 0 \quad (54)$$

$$v(t_0) < |\nu(t_0)| \geq 2v(t_0) \quad (55)$$

Further refinements on the choice of $\nu(t_0)$ will be made when fixing the desired second thrusting interval.

With $\nu(t_0)$ established in the range provided by the previous inequalities, the initial value of Ψ can be found such that the switching function exhibits the behavior shown in Fig. 1. The computation of $\Psi(t_0)$ is based upon the principle that the duration of the first thrusting interval is proportional to the ratio of the first and second derivatives of the switching function evaluated at time t_0. In other words

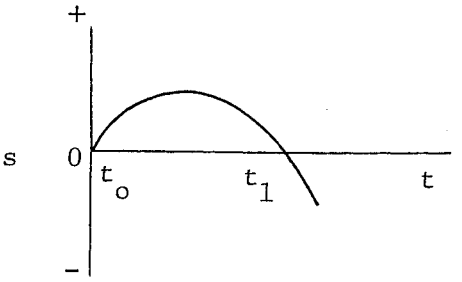

Fig. 1 Desired switching function behavior for the first thrusting interval.

$$(t_1 - t_0) = [-K(\dot{s}/\ddot{s})]_{t=t_0} \quad (56)$$

If s were constant over the time interval $t_0 - t_1$, then the proportionality factor K in the previous equation would be equal to two. The initial true anomaly is determined from the two-impulse trajectory, and a reasonable starting value for $\nu(t_0)$ is selected from the range defined by inequalities Eqs. (53-55). Equation (56) is then solved iteratively for the initial thrust angle using $K = 2$ on the first set of iterations. The system differential equations are then integrated to determine the actual duration of the first thrusting interval. Defining t_{1d} = desired time for termination of the first thrust interval and t_{1a} = termination time of first thrust interval established by integration, then a new value of K is computed according to the following rule:

$$K_{\text{new}} = [1 - (t_{1d} - t_{1a})/(t_{1d} - t_0)]K_{\text{old}} \quad (57)$$

This new value of K is now substituted into Eq. (56), and Eq. (56) is once again solved iteratively for $\Psi(t_0)$. The process is repeated until t_{1a} becomes within a certain tolerance of t_{1d}.

This method of determining $\Psi(t_0)$ has proven very reliable and efficient. In the actual computer program, double-precision arithmetic is used for the iterative solution of Eq. (56), but the integration of the system equations is performed in single-precision arithmetic. For most minimum-fuel problems considered, the difference between t_{1d} and t_{1a} can be made less than 5×10^{-7} time units in 3 or 4 iterations.

The desired duration of the second thrusting interval is attained in an iterative manner through a simultaneous adjustment of $\Psi(t_0)$ and $\nu(t_0)$. This is accomplished by computing $\Psi(t_0)$ to obtain the desired first thrusting interval. For every new value of $\nu(t_0)$, $\Psi(t_0)$ must be recomputed in order to satisfy the requirements of the first thrusting interval.

The specific manner in which $\nu(t_0)$ is changed in order to satisfy the second thrusting interval requirements depends upon the type of transfer trajectory being considered. Transfer trajectories can be classed according to the direction of the thrust vector on each of the thrusting intervals. Let forward and rearward thrustings be defined as thrustings along which the thrust angle is near 0° and 180°, respectively. Then each transfer trajectory can be classed according to the thrusting sequence as forward-rearward, rearward-forward, forward-forward, or rearward-rearward. The duration of the second thrusting interval can be set through a proper choice of $\nu(t_0)$ for each of the previous types of transfer trajectories. However, the manner in which $\nu(t_0)$ affects the switching function in the forward-rearward and rearward-forward transfers is notably different from the forward-forward and rearward-rearward transfers.

Selection of a reasonable $\nu(t_0)$ for forward-rearward and rearward-forward transfers is governed by the requirement

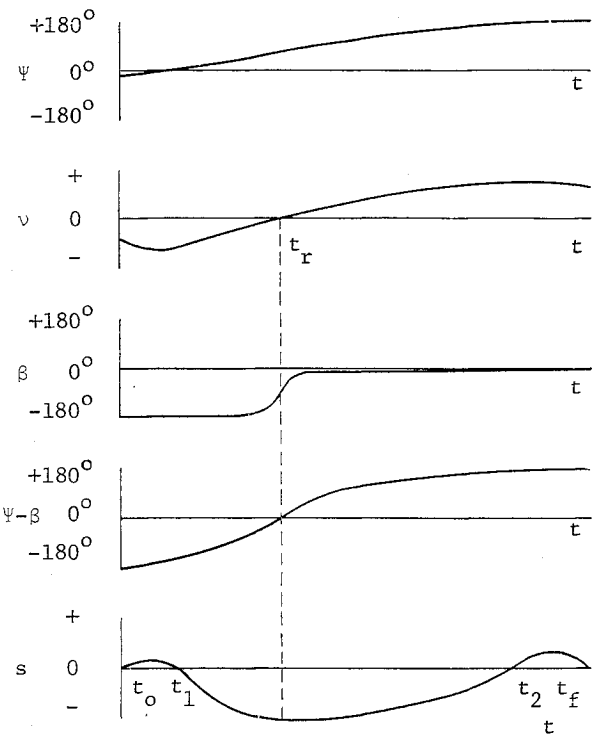

Fig. 2 Typical behavior of Ψ, υ, β, Ψ-β, and the switching function over an entire transfer trajectory for the case of a forward-rearward thrusting sequence.

that the thrust angle must change through approximately 180° along the transfer trajectory. The curves of Fig. 2 can be used to show how switching is accomplished on a typical transfer trajectory with a forward-rearward thrusting sequence. As is evident from the figure, the angle $\Psi - \beta$ is near $\pm 180°$ on both thrusting intervals. Examination of Eqs. (48) and (49) reveals that this requirement on the angle $(\Psi - \beta)$ must always be met if switching is to be accomplished. As is typical of all forward-rearward transfers, the thrust angle increases over most of the trajectory, the variable ν increases monotonically over the entire coast trajectory, and the angle β changes by approximately 180° over the transfer trajectory. In addition, the time t_r at which ν passes through zero corresponds very closely to the time on the coast trajectory at which the slope of the switching function reverses from negative to positive. Since ν increases monotonically along the coast trajectory, the time t_r can be controlled with the initial value of ν. Therefore, a certain amount of control can be exerted upon the switching function by means of $\nu(t_0)$. Larger negative values of $\nu(t_0)$ will result in larger values of time t_r. The value of t_r in turn has a direct effect upon the duration of the second thrusting interval. Larger values of t_r allow the switching function to become more negative on the coast phase. Consequently, because of the particular nature of the switching function dynamics, the duration of the second thrusting interval is decreased. This leads to the important conclusion that the duration of the second thrusting interval can be controlled with $\nu(t_0)$. More negative values of $\nu(t_0)$ result in smaller second thrusting intervals.

Similar reasoning can be applied to the case of rearward-forward transfer. In this case, higher positive values of $\nu(t_0)$ will lead to smaller second thrusting intervals.

Therefore for forward-rearward or rearward-forward thrusting sequences the following iterative procedure for determining the initial value of ν can be formulated. 1) Select an initial, reasonable $\nu(t_0)$. For example, $\nu(t_0) = 1.5v(t_0)$ for rearward-forward thrusting and $\nu(t_0) = -1.5v(t_0)$ for forward-rearward thrusting. 2) Compute $\Psi(t_0)$ such that the correct first thrusting interval is attained. 3) Integrate the system equations to some time $t_f + \Delta t$ sufficient for the transfer to be accomplished. The time t_f can be easily estimated from the two-impulse transfer. 4) Compute the second thrust interval. If this interval is too small, decrease $|\nu(t_0)|$. If too large, increase $|\nu(t_0)|$. 5) Repeat, using the improved value for $\nu(t_0)$, until the actual second thrusting interval duration, as determined from the integration, is within a certain tolerance of the desired second thrusting interval duration.

Using the previous approach, it is possible for most of the transfer trajectories considered in this study to obtain the actual second thrust interval duration to within 5×10^{-5} time units of the desired second thrust interval duration.

For the case of rearward-rearward or forward-forward transfer trajectories, the thrust angle experiences only a small net change over the entire transfer trajectory. In order to restrict the thrust angle in this manner, $\nu(t_0)$ must be chosen very near $-2v(t_0)$ for forward-forward transfers and near $+2v(t_0)$ for rearward-rearward transfers. The value of ν does not change sign along these transfer trajectories. Reversal of the switching function slope and therefore the duration of the second thrusting interval is governed by a very delicate balance between the terms hu and $(h - s)\rho \sin(\Psi - \beta)/\Lambda$ appearing on the right hand side of Eq. (49). A consideration of the switching function behavior for these types of transfers leads to the conclusion that larger absolute values of $\nu(t_0)$ will lead to larger second thrusting interval durations.[8] This fact can be used as a basis to formulate an iterative procedure for establishing the second thrusting interval duration for forward-forward or rearward-rearward transfer trajectories. The basic procedure will be similar to the case of forward-rearward or rearward-forward transfers. However, to start the iteration, $\nu(t_0)$ must be near either $+2v(t_0)$ or $-2v(t_0)$. In addition, as discussed previously, changes in $\nu(t_0)$ will produce the opposite effects upon the duration of the second thrusting interval.

Final Convergence Method

The procedure developed in the previous section results in a transfer trajectory with final boundary conditions which are only reasonably close to the desired boundary conditions. Better matching of the final boundary conditions is achieved by a two-step procedure which is based primarily upon small perturbations about the initial-approximate transfer trajectory developed in the previous section.

The first step in improving the initial-approximate transfer trajectory is to make small adjustments in the initial true anomaly $f(t_0)$ in order to improve the final argument of pericenter $\phi(t_f)$. This is accomplished by computing a sensitivity coefficient which relates small changes in $f(t_0)$ to small changes in $\phi(t_f)$. The resulting sensitivity coefficient is used in a conventional linear interpolation or extrapolation procedure to compute a new $f(t_0)$ which will result in an improved $\phi(t_f)$. After each change in $f(t_0)$, $\Psi(t_0)$ and $\nu(t_0)$ are readjusted as outlined in the previous section in order to maintain the desired thrusting intervals. In the actual computation $f(t_0)$ is adjusted in this manner until $\phi(t_f)$ is within 0.02 rad of the desired value.

Final convergence to the desired transfer trajectory is achieved through the use of a sensitivity matrix which relates small changes in $f(t_0)$, $\Psi(t_0)$, and $\nu(t_0)$ to corresponding changes in the final semilatus rectum $p(t_f)$, final eccentricity $e(t_f)$, and final argument of pericenter $\phi(t_f)$. On the first iteration the sensitivity matrix is computed by perturbing one at a time $f(t_0)$, $\Psi(t_0)$, and $\nu(t_0)$ and observing the resultant changes in $p(t_f)$, $e(t_f)$, and $\phi(t_f)$. Subsequent computations of the sensitivity matrix can be made directly from the two most recent trajectories by employing a method described by Kulakowski and Stancil.[12] The sensitivity matrix computed in this manner is used in the well-known linear algorithm to compute an

improved set of initial conditions, $f(t_0)$, $\Psi(t_0)$, and $\nu(t_0)$. Computation is terminated when the final conditions $p(t_f)$, $e(t_f)$, and $\Psi(t_f)$ are all within 10^{-4} units of their respective desired values.

IV. Computational Techniques

In the process of determining the minimum-fuel transfer trajectory it is necessary to compute transfer trajectories for a relatively large number of starting conditions. In order that the computation be efficient, it is essential that both the total number of transfer trajectories computed and the amount of required computation for each transfer trajectory be kept within reasonable bounds. The techniques which make possible the efficient computation of minimum-fuel trajectories are as follows.

Canonical Transformation on the Coast Trajectory

Computation along the coast trajectory is made possible by means of a canonical transformation suggested by Fraeijs DeVeubeke of the system state variables, adjoint variables and the independent variable t.[9] The independent variable in the newly transformed set is the polar angle θ, and the new set of state variables are z, A, B, w, and t, where z, A, and B have been defined previously in Eqs. (25–27). Along the coast trajectory with this particular transformation H_1, the portion of the Hamiltonian which governs switching, is a function only of the state and adjoint variables at cutoff of the first thrusting interval and the polar angle θ.[9] Computation of the coast phase is accomplished by performing the canonical transformation at the end of the first thrusting interval. Since H_1 must be negative along the entire coast trajectory and equal to zero at the end of coast, the polar angle θ which defines the end of the coast phase is easily established by means of a Newton iteration procedure. To begin the iteration, a reasonable first estimate of the desired polar angle is computed from the corresponding two-impulse transfer trajectory. With the polar angle at the end of coast established in this manner, a transformation back to the original variables is performed and integration of the second thrusting interval is initiated.

Computation of the Thrusting Phases

The two thrusting phases are computed using a fixed step-size, fourth-order Runge-Kutta integration algorithm with single-precision arithmetic. With proper choice of step-size, application of the fixed step-size integration routine rather than an integration routine employing automatic step-size control reduces the required computation time by a factor of about 3. The system Hamiltonian, which must remain zero over the entire transfer trajectory, provides a convenient measure of integration accuracy. Integration step-size is chosen such that the Hamiltonian ordinarily remains less than 5×10^{-7}.

The thrusting phases must be terminated at precisely the instant at which the switching function s passes through zero. This is accomplished by allowing the integration to proceed until the switching function reverses sign and becomes negative. The value of s and $\dot{s}$ are computed at this time, and the integration routine is given a new step-size $(-s/\dot{s})$. This process is repeated until the magnitude of s becomes less than 10^{-7}.

Backward Integration of the System Equations

For certain classes of transfer trajectories, the resulting final values of semilatus rectum, eccentricity, and argument of pericenter become very sensitive to small changes in the program initial conditions. This is particularly true when the second thrusting interval is very small. For this case, it becomes practically impossible to find the set of initial conditions that will allow the switching function to provide proper switching on the second thrusting interval. Very small changes in the initial conditions on the order of 5×10^{-8} result in either too much thrusting time or else no thrusting time for the second thrusting interval. This difficulty is overcome by computing these transfer trajectories in the reverse sense, starting at the desired terminal conditions and integrating backwards in order to meet the desired initial conditions.

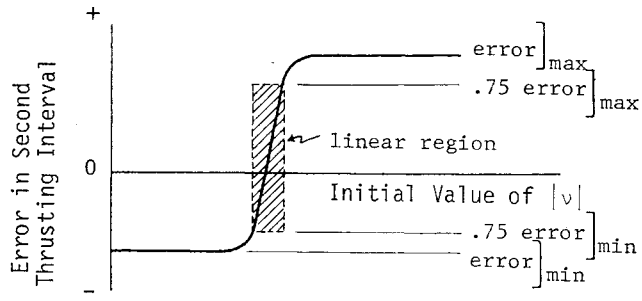

Fig. 3 Error in the duration of the second thrusting interval as a function of the initial value of ν.

Determination of the Initial Value of ν

The initial value of the variable ν is determined so that the desired duration of the second thrusting interval is attained. For most transfer trajectories, the duration of the second thrusting interval is very sensitive to the choice of the initial value of ν. In order to limit computer time, a considerable amount of computation logic is required in establishing the desired initial value of ν. The general behavior of the error in the duration of the second thrusting interval as a function of the initial value of $|\nu|$ is shown in Fig. 3 for the case of a forward-rearward transfer trajectory. The maximum error in Fig. 3 is a consequence of the initial $|\nu|$ being too large. This causes the switching function s to remain negative on the desired second thrusting interval resulting in a complete absence of the second thrusting interval. On the other hand, the minimum error is caused by the initial value of $|\nu|$ being too small. This results in a failure of the switching function to return to zero on the second thrusting interval and therefore, the thrusting interval is not terminated.

The basic computational problem is to find the initial value of ν that reduces the duration error to a small value without requiring an unreasonable number of trajectory computations. Therefore, in the early stages of the computation, large changes in the initial value of ν are programmed in order to establish quickly the minimum and maximum error bounds. Once these two error bounds have been established, linear interpolation between these bounds is employed, with the restriction that the interpolation always be conducted between the values of positive and negative error. This procedure is followed until two initial values of ν can be found for which the errors lie within a region with upper and lower bounds of 0.75 $\times$ (maximum error) and 0.75 $\times$ (minimum error), respectively. From this point on in the computation, linear interpolation or extrapolation is conducted between the two most recent pairs of initial ν and error values. Computation is terminated when the duration of the second thrusting interval is within 10^{-4} time units of the desired duration.

V. Numerical Results

In order to define the limits of applicability of the method and to eliminate any serious deficiencies in the computer

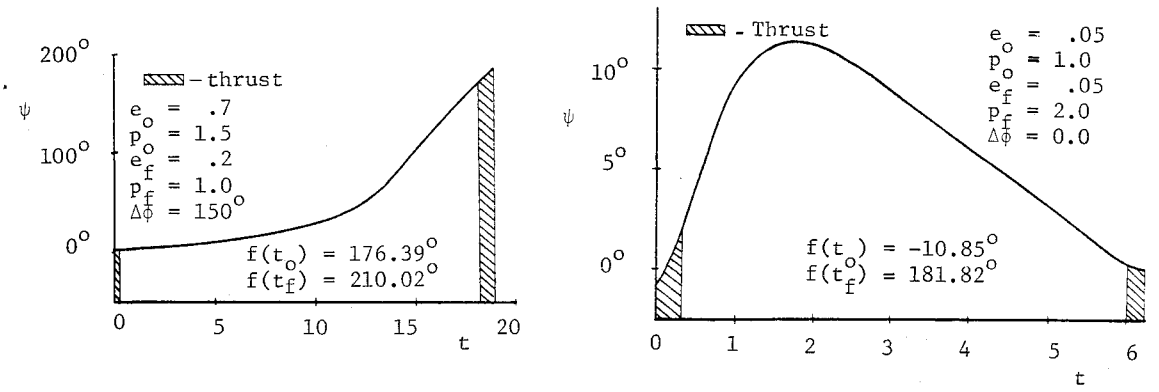

a) forward-rearward thrusting **b) forward-forward thrusting**

Fig. 4 Typical thrust-angle time histories along the minimum-fuel transfer trajectory.

program, a large number of different transfer trajectories were considered. Six of these trajectories are summarized in Table 1. An effective exhaust velocity c of 0.5 is used for all the transfer trajectories. If the basic unit of length is taken as the Earth's radius, this effective exhaust velocity is equivalent to a specific impulse of approximately 400 sec. A transfer trajectory is considered to be convergent if the errors in the final (in the case of forward computation) or initial (in the case of backward computation) eccentricity, semilatus rectum, and argument of pericenter (radians) are each less than 10^{-4}. All of the transfer trajectories in Table 1 are convergent by the above definition.

The thrust angle behavior for runs 1 and 2 of Table 1 is shown in Fig. 4. Also included are the initial and final true anomalies. The forward-rearward transfer, Fig. 4a, is typified by the thrust angle changing by approximately 180° along the transfer trajectory, while in the case of the forward-forward thrusting sequence (Figure 4b) the thrust angle experiences only a very small net change over the entire transfer trajectory. Figure 4b shows the thrust angle behavior for the transfer between almost circular orbits ($e_0 = e_f = 0.05$). The thrust angle behavior and the initial and final true anomalies bear close resemblances to the minimum-fuel two-impulse transfer between circular orbits, better known as the Hohmann transfer.

IBM 7094 computer time requirements ranged from a low of 10 sec to a high of about 50 sec, with the higher computer times being associated with transfer trajectories, which are very sensitive to small changes in the initial conditions. The aforementioned times are for the finite-thrust transfer trajectory computation only. Approximately 20 additional seconds of computer time are required for the computation of the corresponding minimum-fuel two-impulse transfer trajectory. A detailed computer time breakdown for the trajectories summarized in Table 1 is shown in Table 2. The run numbers appearing in the table are consistent with Table 1. Computer time is given in seconds.

The individual errors in the desired semilatus rectum, eccentricity, and argument of pericenter for run 5 of Table 1 are given in Table 3 as a function of the iteration number.

Table 1 Summary of minimum-fuel transfer trajectories

Run	a	$e(t_0)$	$p(t_0)$	$e(t_f)$	$p(t_f)$	$\Delta\phi$ deg	Finite thrust ΔV	Two impulse ΔV
1	0.4	0.7	1.5	0.2	1.0	150	0.3635435	0.3622068
2	0.4	0.05	2.0	0.05	1.0	0	0.2803388	0.2802910
3	0.05	0.2	1.25	0.2	1.50	120	0.1462795	0.1424484
4	0.4	0.2	1.50	0.8	1.0	90	0.3050198	0.3048221
5	0.4	0.03	1.25	0.2	1.5	120	0.0920852	0.0920252
6	0.4	0.05	1.0	0.05	2.0	0	0.2807767	0.2805122

This particular transfer trajectory is computed in a backward sense, starting at the desired final conditions and attempting to match the desired initial conditions. The low initial eccentricity $e_0 = 0.03$ results in rapid changes in the argument of pericenter as the initial orbit is approached. This causes the argument of pericenter error to be relatively large, thus slowing down the convergence. The errors corresponding to iteration zero are the errors for the initial-approximate transfer trajectory. On iterations 1–4 the initial true anomaly $f(t_0)$ is adjusted to reduce the argument of pericenter error. Iteration one obtains the initial sensitivity, relating changes in $f(t_0)$ to changes in argument of pericenter error. The true anomaly $f(t_0)$ is increased arbitrarily by 0.01, and $\Psi(t_0)$ and $\nu(t_0)$ are recomputed to attain the required thrusting interval durations. At the end of iteration 4, the argument of pericenter error is less than the pre-established maximum value of 2×10^{-2}, and the simultaneous adjustment of $f(t_0)$, $\Psi(t_0)$, and $\nu(t_0)$ by means of the sensitivity matrix is initiated. Computation is terminated at the end of iteration 12 with the errors all less than 10^{-4}.

The region of applicability of the convergence method cannot be precisely defined because of the many possible combinations of rocket thrust levels and initial and final orbits. Minimum-fuel transfer trajectories have been successfully computed for orbital eccentricities greater than 10^{-8} and less than 0.8 and for rocket thrust to weight ratios greater than 0.025 and less than 1.0. Convergence is more difficult to attain for trajectories with forward-forward or rearward-rearward thrusting sequences. This is primarily because of the delicate balance which must be maintained between the terms $(h - s)\rho \sin(\Psi - \beta)/\Lambda$ and hu of Eq. (49) in order to obtain the desired switching function characteristics. Both of these terms remain very small and are of opposite sign over most of the transfer trajectory. This results in very small changes in the switching function over the entire transfer trajectory.

Table 2 Computation time (IBM-7094)

Run	Phase time, sec: Phase I[a]	Phase II[b]	Phase III[c]	Total time, sec
1	4	5	2	11
2	8	10	3	21
3	7	6	2	15
4	9	14	4	27
5	4	9	3	16
6	7	36	2	45

[a] Phase I—initial approximate transfer trajectory.
[b] Phase II—adjustment of initial true anomaly.
[c] Phase III—final convergence (sensitivity matrix).

Table 3 Error behavior (run 5, Table 1)

Iteration	Error × 10^3		
	p	e	ϕ, rad
0	1.17368	−22.87911	329.30260
1	1.12581	−25.11474	349.50271
2	−0.16358	1.88112	−45.97852
3	0.00699	−1.03564	29.97921
4	−0.03710	0.04818	1.08311
5	−0.15672	0.09923	2.11155
6	0.01580	0.00327	−0.88245
7	−0.04964	0.02363	1.04833
8	−0.01092	0.00512	0.23766
9	−0.00547	0.00264	0.12189
10	−0.02010	0.00963	0.41148
11	−0.01302	0.00654	0.29120
12	−0.00454	0.00227	0.09516

VI. Conclusion and Future Study

An efficient method for computing time-open minimum-fuel finite-thrust transfer trajectories between two given coplanar elliptic orbits has been developed. Computation of the minimum-fuel transfer trajectory is accomplished by a direct integration of the rocket equations and the associated adjoint equations. This direct approach is made possible through the insight gained from a transformation of the adjoint equations.

The program has been extended recently to make the convergence method applicable to a larger class of transfer trajectories.[13] A finite-thrust correction developed by Robbins was applied to the thrusting intervals during computation of the initial-approximate transfer trajectory.[14] This correction forced the initial-approximate transfer trajectory closer to the desired transfer trajectory. This has extended convergence to lower thrust levels and to transfers requiring higher impulse levels. In addition, a method was developed to compute an initial estimate of $\nu(t_0)$ directly from the two-impulse program. This has improved convergence particularly at higher orbital eccentricities. Also, the entire method was programmed in double precision arithmetic. This has increased the accuracies at every stage of the computation, thus extending the method to include more sensitive transfers.

References

[1] McCue, G. A., "Quasilinearization Determination of Optimal Finite-Thrust Orbital Transfers," *AIAA Journal*, Vol. 5, No. 4, April 1967, pp. 755–763.

[2] Handelsman, M., "Optimal Free-Space Fixed-Thrust Trajectories Using Impulsive Trajectories as Starting Iteratives," *AIAA Journal*, Vol. 4, No. 6, June 1966, pp. 1077–1082.

[3] Lee, G., "An Analysis of Two-Impulse Orbital Transfer," *AIAA Journal*, Vol. 2, No. 10, Oct. 1964, pp. 1767–1773.

[4] McCue, G. A. and Bender, D. F., "Numerical Investigation of Minimum Impulse Orbital Transfers," *AIAA Journal*, Vol. 3, No. 12, Dec. 1965, pp. 2328–2334.

[5] Kern, E. A. and Burghart, J. H., "An Efficient Algorithm for Minimum Impulse Orbital Transfer," *AIAA Journal*, Vol. 6, No. 7, July 1968, pp. 1370–1372.

[6] Robbins, H. M., "Optimality of Intermediate-Thrust Arcs of Rocket Trajectories," *AIAA Journal*, Vol. 3, No. 6, June 1965, pp. 1094–1098.

[7] Kopp, R. E. and Moyer, H. G., "Necessary Conditions for Singular Extremals," *AIAA Journal*, Vol. 3, No. 8, Aug. 1965, pp. 1439–1444.

[8] Kern, E. A., "Minimum-Fuel Thrust-Limited Transfer Trajectories Between Coplanar Elliptic Orbits," Ph.D. thesis, 1968, The Univ. of Michigan, Ann Arbor, Mich.

[9] Fraeijs DeVeubeke, B., "Canonical Transformations and the Thrust-Coast-Thrust Optimal Transfer Problem," *Astronautica Acta*, Vol. 11, No. 4, July-Aug. 1965, pp. 271–282.

[10] Fraeijs DeVeubeke, B., "Optimal Steering and Cutoff-Relight Programs for Orbital Transfer," *Astronautica Acta*, Vol. 12, No. 4, July-Aug. 1966, pp. 323–328.

[11] Culp, R. D., "Contenson-Buseman Conditions for Optimal Coplanar Orbit Transfer," *AIAA Journal*, Vol. 5, No. 2, Feb. 1967, pp. 371–372.

[12] Kulakowski, L. J. and Stancil, R. T., "Rocket Boost Trajectories for Maximum Burnout Velocity," *ARS Journal*, Vol. 30, No. 7, July 1960, pp. 612–618.

[13] Gill, D. E. and Wambold, G. D., "Improved Initial Value Estimates For Minimum-Fuel Orbital Transfers," M.S. thesis, GGC/EE/69-9, 1969, The Air Force Institute of Technology, Wright-Patterson Air Force Base, Ohio.

[14] Robbins, H. M., "An Analytic Study of the Impulsive Approximation," *AIAA Journal*, Vol. 4, No. 8, Aug. 1966, pp. 1417–1423.